Model Predictive Control for Torque Ripple Suppression Caused by Misalignment of the Gearbox

Soo-Hwan Park, Jin-Cheol Park, Sung-Woo Hwang, Jae-Hyun Kim, and Myung-Seop Lim, *Member, IEEE*

***Abstract*—This paper presents a model predictive control (MPC) based harmonic current injection method (HCIM) to suppress the torque ripple caused by misalignment in gearbox. As it is inefficient to determine the amplitude and phase of harmonic currents manually, the MPC is used to search the appropriate harmonic currents to implement HCIM efficiently. A cost function for MPC is designed to minimize a resultant torque ripple which is calculated by summing the misalignment torque ripple and compensation torque. The compensation torque is an input variable of the predictive model. In order to predict the resultant torque ripple accurately, an estimation method of the misalignment torque ripple with torque sensor is also proposed. The calculated compensation torque is converted into harmonic currents and the harmonic currents can be injected into a *q*-axis current. As a result, the misalignment torque ripple can be suppressed. Experimental results demonstrate verification for estimation method of misalignment torque ripple, and effectiveness of the HCIM. In addition, the proposed MPC-HCIM is also verified by experiments, and the misalignment torque ripple is effectively suppressed by using the proposed method. By using the proposed method, high degree of precision in torque control can be achieved with low quality gearbox which has misalignment.**

***Index Terms*—Gearbox, harmonic current injection method, misalignment, model predictive control, torque ripple.**

I. Introduction

THE surface-mounted permanent magnet synchronous motor (SPMSM) is widely used in industrial applications such as multi-axis robot because of its convenience in control, low torque ripple, and high power density [1]. Since the control scheme of field-oriented control (FOC) is adopted for SPMSM, the electromagnetic torque of the SPMSM can be controlled linearly by using *q*-axis current [2]. Because of its sinusoidal flux-linkage, the SPMSM can produce electromagnetic torque with low torque ripple. Therefore, the industrial applications adopts the SPMSM for its low electromagnetic torque ripple.

Generally, the electromagnetic torque is transferred to the load through the gearbox because the industrial applications consist of the SPMSM and gearbox. Although the SPMSM generates low electromagnetic torque ripple, large torque ripple is transmitted to the load because of the torque ripple caused by the gearbox. It is necessary to reduce the torque ripple because it degrades the precision of the torque control, and it is a source of torsional vibration [3]. The main factor of the torque ripple is shaft misalignment caused by manufacturing tolerances, and the misalignment produces the preload forces which affects to the friction torque and torque ripple. Thus, the friction torque can be increased with fluctuating torque ripple because of the misalignment. The misalignment can be reduced by controlling the manufacturing tolerances. However, it requires high costs to control the manufacturing tolerances. Therefore, it is efficient to suppress the torque ripple by using control methods.

The misalignment torque ripple, which is caused by the shaft misalignment, acts as a nonlinear element in actuator control. A number of methods for model-based friction torque compensation have been proposed such as LuGre model-based methods [5], [6]. On the other hand, the reduction of electromagnetic torque ripple has been studied by the design method of the motor [7], [8] and the compensation control method [9]. However, these methods only considered the averaged friction torque and electromagnetic torque ripple, but the friction and torque ripple caused by the gearbox have not been considered. To consider the misalignment torque ripple, compensation methods using a torque sensor have been proposed [10], [11]. The methods enables high accuracy control but the torque sensor requires high cost and maintenance.

In this view, we propose a control method for suppressing the misalignment torque ripple without any torque sensor. To suppress the misalignment torque ripple, a harmonic current injection method (HCIM) is adopted in this paper. The HCIM has been widely used as a method for suppressing electromagnetic torque ripple by injecting harmonic current into the armature current [14]–[16]. HCIM is effective to eliminate electromagnetic torque ripple, but the aforementioned studies have not considered misalignment torque ripple. A method for reducing misalignment torque ripple using HCIM has been proposed [17]. The method enables to suppress the misalignment torque ripple by injecting the harmonic currents into the *q*-axis current to generate the compensation torque which has opposite phase with the misalignment torque ripple. However, the method is difficult to use universally because there is no controller for determining the amplitude and phase of harmonic current.

Manuscript received April 21, 2020; revised September 26, 2020 and February 1, 2021; accepted February 12, 2021. Date of publication February 19, 2021; date of current version May 21, 2021. This work was supported by the National Research Foundation of Korea funded by the Korea government (Ministry of Science, ICT & Future Planning) under Grant 2018R1C1B5085447. Paper no. TEC-00399-2020. *(Corresponding author: Myung-Seop Lim.)*

The authors are with the Department of Automotive Engineering, Hanyang University, Seoul 04763, Republic of Korea (e-mail: shwanp14@hanyang.ac.kr; skensk1990@hanyang.ac.kr; supertramph@hanyang.ac.kr; zerg1258@hanyang.ac.kr; myungseop@hanyang.ac.kr).

Color versions of one or more figures in this article are available at https://doi.org/10.1109/TEC.2021.3060536.

Digital Object Identifier 10.1109/TEC.2021.3060536

Generally, the control method of PI control is used to determine the amplitude and phase of the harmonic currents. Thanks to the flexibility of cost function in model predictive control (MPC), MPC is efficient because it can calculate the amplitude and phase of each harmonic components simultaneously by designing the cost function. However, the PI controller must be designed separately for each harmonic order, so that it is inefficient as the number of harmonic components increases [18]. In addition, the PI gain needs to be tuned according to the load torque and rotating speed while the model predictive control (MPC) needs no tuning process [19]. Therefore, the MPC is used to implement the HCIM in this paper.

The MPC is a method of controlling the variables by determining the input variables to minimize the cost function. The cost function is evaluated according to the predicted control variables which is calculated by using predictive model and input variables. Therefore, it is important to design the predictive model accurately to use the MPC effectively. The MPC has been widely used for controlling variables such as current, voltage, or speed of electro-mechanical applications. Among them, Kouro *et al.* and Aguilera *et al.* have been used the MPC to eliminate specific harmonic voltages in power converter applications [21], [22]. They designed the cost function by using the amplitude of each harmonic voltage to reduce the specific harmonic component. Likewise, the harmonic components of the misalignment torque ripple can be selectively suppressed by designing the cost function using sum of the misalignment torque ripple and compensation torque rather than voltage harmonics in this paper. Since the bandwidth of the mechanical system is relatively low compared to the power converter applications, this paper proposes a process to predict misalignment torque ripple instead of using the torque sensor. Therefore, the proposed combined MPC based HCIM (MPC-HCIM) method is suitable for suppressing the misalignment torque ripple because the cost function can be designed flexibly by using various harmonic components.

In this contribution, the misalignment torque ripple is suppressed by using MPC-HCIM. In order to implement the MPC-HCIM, the amplitude and phase of the misalignment torque ripple have to be estimated first. Thus, the estimation method of the misalignment torque ripple without any torque sensor is presented in this paper. Then, the misalignment torque ripple can be suppressed by injecting the harmonic currents which have appropriate amplitude and phase. Using the proposed method, a high degree of precision in torque control can be achieved despite the use of gearbox with the misalignment.

II. The Effect of Misalignment on Torque Ripple

A. Rotor Dynamics by the Misalignment Torque Ripple

The shaft misalignment is a common problem in manufacturing process of rotating machinery. Fig. 1(a) and Fig. 1(b) show the configuration of the actuator that is used in this study. The actuator consists of the SPMSM, gearbox, and position sensors, and the gearbox consists of planetary gear and helical gear. Since the gearbox is composed of several shafts, the manufacturing tolerances of each shaft accumulate, resulting in misalignment

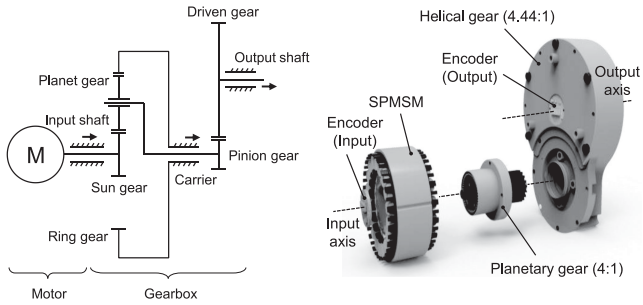

Fig. 1. Configuration of the actuator. (a) Schematic diagram of the actuator, and (b) exploded view of the actuator.

of the gearbox. Thus, the misalignment torque ripple inevitably occurs in the gearbox.

The load is driven by the output torque, which is the electromagnetic torque amplified by the gearbox. Since the electromagnetic torque includes torque ripple due to electromagnetic phenomena, it can be modeled as the sum of averaged torque and torque ripple as

$$T_e = \bar{T_e} + \sum_n T_{e,n} \cos\left(nN_g\theta_{out} + \phi_{e,n}\right) \tag{1}$$

where T_e is the electromagnetic torque, $\bar{T_e}$ and $T_{e,n}$ are the averaged torque and amplitude for the *n*-th electromagnetic torque, respectively, n and N_g are the harmonic orders referred in the output shaft and gear ratio, and θ_{out} and $\phi_{e,n}$ are the position of the output shaft and phase offset for the *n*-th electromagnetic torque, respectively.

When the output torque overcomes the load torque and the rotating machinery is accelerated, friction torque is generated by friction in bearing, fluid friction between air in the air-gap and rotor, and the gears constituting the gearbox. The friction torque can be affected by the shaft misalignment because it causes the preload forces which are divided into static and dynamic force. The static force can be converted into the friction force, and the dynamic force can be converted into the torque ripple which fluctuate periodically as the shaft rotates [4]. Thus, the friction torque is increased and additional torque ripple is generated when the shaft misalignment occurs as shown in Fig. 2(a) and Fig. 2(b). Despite of using the SPMSM with low electromagnetic torque ripple, a large torque ripple is transmitted to the load due to the friction torque ripple. The harmonic orders of the friction torque ripple are equivalent to the multiples and its sideband of the fundamental component of output shaft speed [23], [24]. Then, the friction torque can be expressed as

$$T_f = B\bar{\omega}_{out} + B\sum_n \omega_{out,n} \cos\left(n\theta_{out} + \phi_{f,n}\right) \tag{2}$$

where T_f is the friction torque, B is the friction coefficient, $\bar{\omega}_{out}$ and $\omega_{out,n}$ are the averaged rotating speed and rotating speed for *n*-th harmonic order of output shaft, respectively, and $\phi_{f,n}$ is the phase offset of the friction torque for *n*-th harmonic order. Then, the dynamic motion of the actuator system referred in the

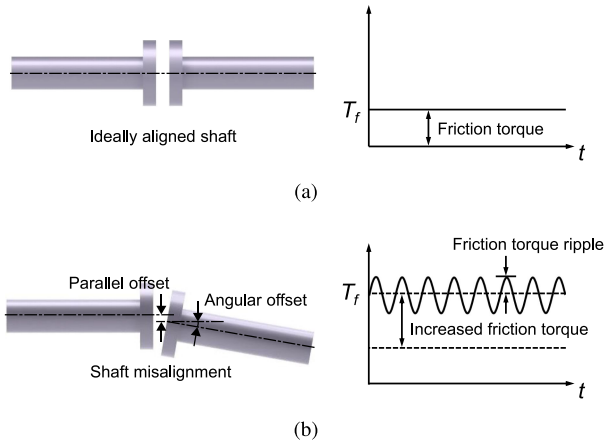

Fig. 2. Effect of the shaft misalignment on friction torque. (a) Friction torque with ideally aligned shaft, and (b) increased friction torque and friction torque ripple with misaligned shaft.

output shaft can be expressed as

$$T_e N_g = J_{eq}\frac{d\omega_{out}}{dt} + T_f + T_L \tag{3}$$

where J_{eq} is the equivalent moment of inertia referred to the output shaft, ω_{out} is the rotating speed of output shaft, and T_L is the load torque. Therefore, the acceleration of the rotating shaft can be determined by the friction torque ripple and electromagnetic torque ripple when the averaged electromagnetic torque and load torque are constantly controlled.

B. Estimation of the Misalignment Torque Ripple Without Torque Sensor

It is necessary to measure the misalignment torque ripple because the proposed MPC-HCIM starts with measuring the torque ripple. The torque ripple can be measured accurately by using a torque sensor, but it is not efficient that the torque sensor requires extra cost and maintenance. Thus, the method for estimating the misalignment torque ripple without torque sensor is proposed in this paper.

Since the SPMSM is controlled by the FOC algorithm, the SPMSM can be modeled based on the *d, q*-axis and the electromagnetic torque can be expressed as

$$T_e = 1.5P_n\left\{\psi_a i_{oq} + (L_d - L_q)\, i_{od} i_{oq}\right\} \tag{4}$$

where the subscripts of d and q are the *d, q*-axis, P_n is the pole-pair, i_{od} and i_{oq} are the magnetization currents, L_d and L_q are the inductances. Since the FOC control method of '$i_d = 0$' is adopted, the electromagnetic torque can be written as

$$T_e = 1.5P_n\psi_a i_{oq} \tag{5}$$

However, the current controller controls the *d, q*-axis current, not the magnetization current because the magnetization current cannot be measured directly. As the *d, q*-axis currents are the sum of magnetization current and iron loss current, the *d, q*-axis current can be expressed as

$$i_d = i_{od} + i_{cd},\;\; i_q = i_{oq} + i_{cq} \tag{6}$$

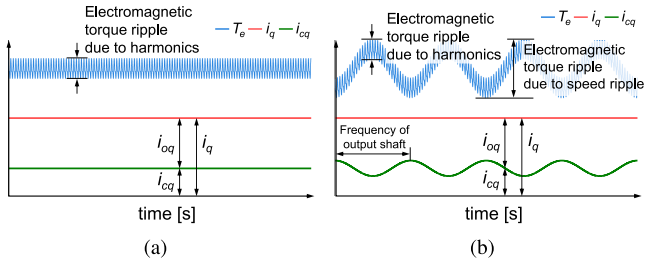

Fig. 3. Effect of the shaft misalignment on electromagnetic torque when the q-axis current is constantly controlled. Electromagnetic torque and q-axis current without shaft misalignment and (b) with shaft misalignment.

where i_d and i_q are the *d, q*-axis currents, and i_{cd} and i_{cq} are the *d, q*-axis iron loss currents. Then, the electromagnetic torque can be determined by the q-axis current and iron loss current as

$$T_e = 1.5P_n\psi_a\left(i_q - i_{cq}\right) \tag{7}$$

If the shaft is ideally aligned, there will be no fluctuation in rotating speed. Then, the q-axis magnetization and iron loss currents are constant because the iron loss is dependent on the frequency of the magnetic flux density as shown in Fig. 3(a). However, the iron loss current may be changed when the rotating speed contains harmonic component due to the shaft misalignment even if the q-axis current is controlled constantly. As the fluctuated rotating speed causes the variation in iron loss, the electromagnetic torque contains torque ripple also because of the variation in q-axis magnetization current as shown in Fig. 3(b).

If the averaged rotating speed is in a steady-state, the averaged output torque and the sum of the averaged friction and load torque are identical. Then, the acceleration is fluctuated by the electromagnetic torque ripple and friction torque ripple as

$$\frac{d\omega_{out}}{dt} = \frac{1}{J_{eq}}\left\{N_g\sum_n T_{e,n}\cos\left(nN_g\theta_{out} + \phi_{e,n}\right) - B\sum_n \omega_{out,n}\cos\left(n\theta_{out} + \phi_{f,n}\right)\right\} \tag{8}$$

Since the acceleration is a time derivative of the rotating speed, the rotating speed contains the same harmonic components with the acceleration. In this study, the misalignment torque ripple is defined as the sum of electromagnetic torque ripple and friction torque ripple as

$$T_{mis} = N_g\sum_n T_{e,n}\cos\left(n\theta_{out} + \phi_{e,n}\right) - B\sum_n \omega_{out,n}\cos\left(n\theta_{out} + \phi_{f,n}\right) \tag{9}$$

Then, the misalignment torque ripple can be rewritten as

$$T_{mis} = \sum_n T_{mis,n}\cos\left(n\theta_{out} + \phi_{mis,n}\right) \tag{10}$$

where T_{mis} and $T_{mis,n}$ are the misalignment torque ripple and the torque ripple for n-th harmonic order, and the $\phi_{mis,n}$ is the phase offset of the misalignment torque ripple for n-th harmonic order. Since the misalignment torque ripple is composed of

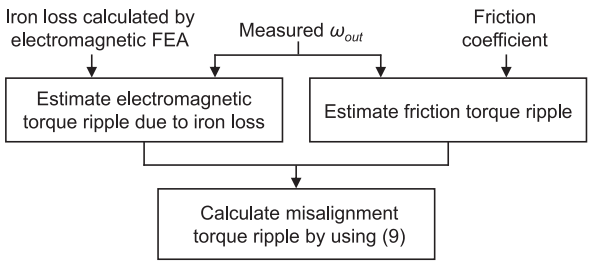

Fig. 4. Process for estimating misalignment torque ripple.

friction and misalignment torque ripple due to the speed fluctuation, it is calculated as zero in normal operation without shaft misalignment. In order to predict the misalignment torque ripple, the iron loss according to the rotating speed should be calculated. As the iron loss is determined by the frequency and magnitude of the magnetic flux density, the misalignment torque ripple can be determined by the rotating speed and q-axis current.

Fig. 4 shows the process of estimating the misalignment torque ripple. As the electromagnetic torque ripple of the SPMSM can be negligible, the electromagnetic torque ripple caused by the iron loss is only considered. The iron loss is calculated by using electromagnetic finite element analysis (FEA). Then, the electromagnetic torque ripple can be estimated by using the calculated iron loss and measured rotating speed. In addition, the friction torque ripple can be estimated by using the friction coefficient and measured rotating speed. Consequently, the misalignment torque ripple can be estimated by using (9) without any torque sensor.

III. Torque Ripple Suppression Based on Model Predictive Control

A. Proposed MPC Based HCIM

The block diagram of the classical control scheme is shown in Fig. 5. The feedback variables such as three-phase currents, and rotor position are interfaced to the digital signal processor (DSP) through analog-to-digital (ADC) channels. The classical control scheme of FOC algorithm is adopted for calculating the voltage vector to control the switching device. The measured three-phase currents are converted into the *d, q*-axis currents by using *d, q*-axis transform and transferred to the current controller. The current controller calculates the *d, q*-axis reference voltage by using PI controller with the reference and measured currents. Then, the armature current flows through the stator windings as the switching device is operated by the reference voltages. As a result, the electromagnetic torque is generated by the interaction between the stator currents and field flux.

Fig. 6 shows the overall control scheme of the proposed method for suppressing the misalignment torque ripple. In addition to the classical control scheme, the MPC-HCIM for suppressing the misalignment torque ripple is implemented. The output variable of the MPC-HCIM is compensation current which is defined as sum of the harmonic currents. The detailed procedure of the HCIM and MPC are presented in following subsections.

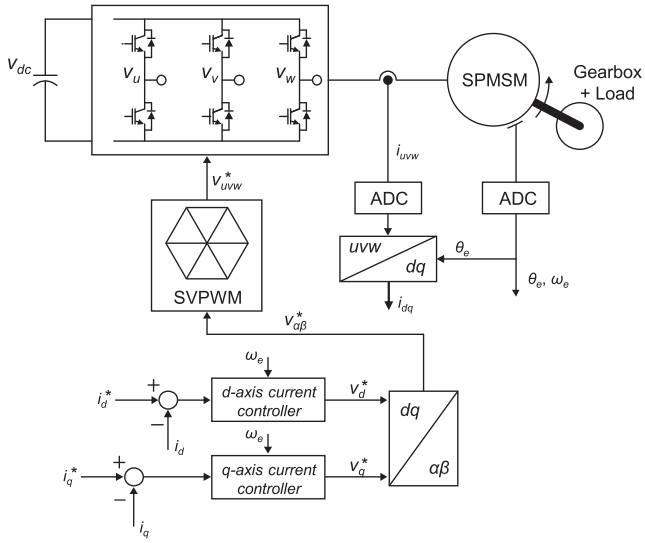

Fig. 5. Classical control scheme of the actuator based on field oriented control.

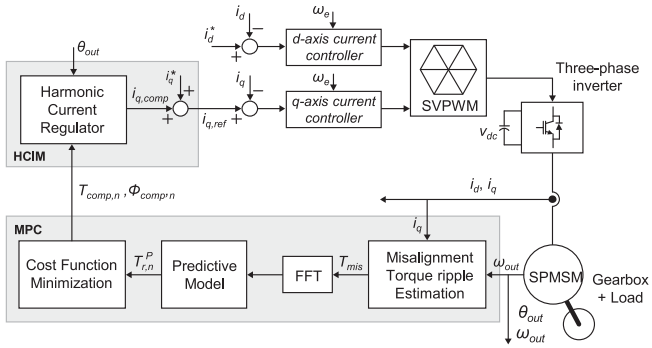

Fig. 6. Proposed model predictive control based harmonic current injection method for suppressing the misalignment torque ripple.

B. Model Predictive Control for Controlling Harmonic Current

Generally, MPC strategy is operated based on discrete time model with sampling frequency. The process of measurement, prediction, and cost minimization should be completed in a single periodic cycle. Therefore, a high bandwidth MPC controller is required for power converter applications [21], [22]. However, the MPC-HCIM depends on the frequency resolution of fast Fourier transform (FFT) because the proposed method is based on the HCIM with FFT. The frequency resolution is determined by the sampling frequency and the data size for FFT [25], and the frequency resolution can be expressed as

$$\Delta f = \frac{f_s}{N_{FFT}} \tag{11}$$

where Δf is the frequency resolution, f_s is the sampling frequency, and the N_{FFT} is the size of the FFT. In this paper, the frequency resolution is set to 0.01 Hz to consider the harmonic order of torque ripple in detail, and the sampling frequency is set to 20 Hz because the frequency of the misalignment torque ripple is very low. After the frequency resolution and sampling

frequency are set to be constant, the size of FFT and total sampling time are determined by using (14). Since the frequency of misalignment torque ripple is low compared to current control period, the effect of current control delay can be negligible. The three steps for MPC-HCIM are as follows: measurements, prediction, and cost minimization.

1) Measurements : The first step for MPC-HCIM is to measure the misalignment torque ripple. Since the misalignment torque ripple can be estimated by using output rotating speed, iron loss, and (9), the output rotating speed and iron loss have to be measured. However, the iron loss cannot be measured directly, so that the iron loss is calculated by using electromagnetic FEA. Since the iron loss depends on the q-axis current and rotating speed, the q-axis current and rotating speed should be measured. The measurement procedure is equivalent to the process of measuring variables using ADC channel in classical control scheme. Then, the measured variables are transmitted to the predictive model, and the resultant torque ripple which is calculated by summing the misalignment torque ripple and compensation torque can be predicted for cost minimization.

2) Prediction : The resultant torque ripple is predicted by using the predictive model for evaluating the cost according to the input variables. Since the resultant torque ripple is determined by the compensation torque, the amplitude and phase of the compensation torque for each harmonic component are selected as input variables. The compensation torque can be expressed as

$$T_{comp} = \sum_{n} T_{comp,n} \cos\left(n\theta_{out} + \phi_{comp,n}\right) \tag{12}$$

where T_{comp} is the compensation torque, $T_{comp,n}$ is the amplitude for n-th harmonic order, and $\phi_{comp,n}$ is the phase offset for n-th harmonic order. When the compensation torque is injected, the dynamic motion of the actuator can be expressed as

$$T_e N_g + T_{comp} = J_{eq}\frac{d\omega_{out}}{dt} + T_f + T_L \tag{13}$$

As it is assumed that the output torque and the sum of the averaged loss torque and load torque are identical, the moment of inertia is accelerated by the sum of the misalignment torque and compensation torque as

$$J_{eq}\frac{d\omega_{out}}{dt} = \sum_{n}\{T_{comp,n}\cos\left(n\theta_{out} + \phi_{comp,n}\right) - T_{mis,n}\cos\left(n\theta_{out} + \phi_{mis,n}\right)\} \tag{14}$$

Then, the predicted resultant torque ripple is calculated as

$$T_r^P = \sum_{n} T_{r,n}^P \cos\left(n\theta_{out} + \phi_{r,n}\right) \tag{15}$$

where

$$T_{r,n}^P = \{T_{comp,n}^2 + T_{mis,n}^2 - 2T_{comp,n}T_{mis,n}\cos\left(\phi_{comp,n} - \phi_{r,n}\right)\}^{-\frac{1}{2}} \tag{16}$$

where $T_{r,n}^P$ is predicted resultant torque ripple for n-th harmonic order, $\phi_{r,n}$ is the phase offset of each predicted resultant torque ripple for n-th harmonic order.

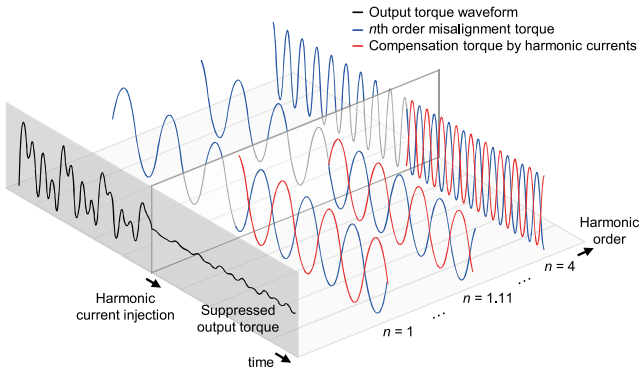

Fig. 7. Principle of the harmonic current injection method.

3) Cost minimization : As a final step of MPC-HCIM, the cost should be minimized for suppressing the misalignment torque ripple. The cost is design as the sum of absolute differences between the reference resultant torque ripple and predicted resultant torque ripple for each harmonic order as

$$g = \sum_{n}\left|\hat{T}_{r,n} - T_{r,n}^P\right| \tag{17}$$

where g and $\hat{T}_{r,n}$ are the cost and reference resultant torque ripple for n-th harmonic order. The reference resultant torque ripple for each harmonic component is set to be zero because the purpose of the proposed method is suppressing misalignment torque ripple completely. Then, the cost of each harmonic component can be minimized when the predicted resultant torque ripple is calculated as zero. As a result, the optimized compensation torque of each harmonic order is determined to have the same amplitude and opposite phase to the misalignment torque ripple. Then, MPC is accomplished by delivering the optimal amplitude and phase of compensation torque to HCIM block.

C. Harmonic Current Injection Method for Suppressing Misalignment Torque Ripple

The HCIM is the method for suppressing torque ripple by injecting harmonic currents to generate harmonic torque which have opposite phase with the torque ripple. Generally, this method has been used to reduce the electromagnetic torque ripple due to the harmonic components in flux-linkage. In this paper, the HCIM is used for suppressing misalignment torque ripple instead of the electromagnetic torque ripple.

Fig. 7 shows the principle of HCIM. Since the electromagnetic torque is proportional to the q-axis magnetization current, a torque ripple with specific frequency can be generated when the harmonic current which has the frequency is injected into the q-axis magnetization current. Likewise, a complex waveform of torque ripple can be intentionally generated by injecting several harmonic currents simultaneously into the q-axis magnetization current. However, the harmonic currents have to be injected into the q-axis current because the q-axis magnetization current cannot be controlled directly.

The harmonic current regulator for HCIM is shown in Fig. 8. The compensation current is calculated by using the harmonic

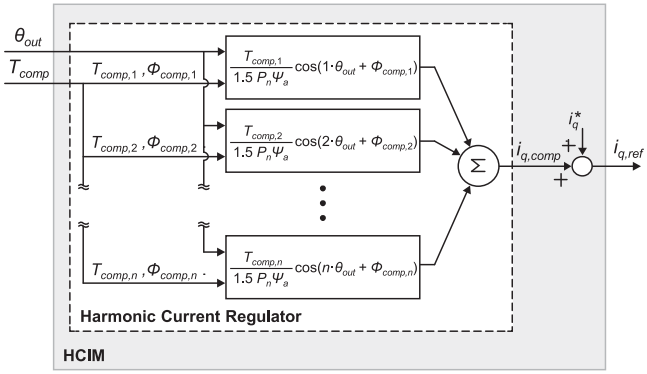

Fig. 8. Configuration of the harmonic current regulator for HCIM.

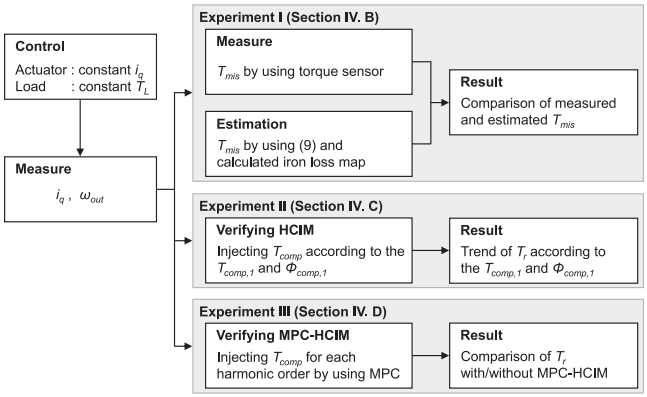

Fig. 9. Flow chart of the experimental verification for proposed MPC-HCIM.

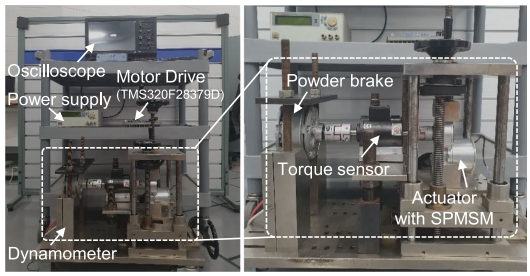

Fig. 10. Experimental setup for MPC-HCIM.

TABLE I
THE SPECIFICATIONS OF THE ACTUATOR

Item	Unit	Value
Number of poles	-	16
Number of slots	-	18
DC link voltage	V	24
Max. power	W	100
Rated torque (Output)	Nm	8
Max. speed (Output)	rpm	65
Overall gear ratio	-	16.44:1
Equivalent moment of inertia	kg·m^2	0.00269
Phase resistance (R_a)	Ω	0.58
d-axis inductance (L_d)	mH	1.44
q-axis inductance (L_q)	mH	1.47
Flux-linkage (ψ_a)	Wb	0.024
Friction coefficient	Nm·s/rad	0.03654
Encoder resolution	bit	12

current regulator. The amplitude and phase of compensation torque are transferred from the results of MPC, and the compensation harmonic currents are calculated by using the relationship between q-axis current and electromagnetic torque of (5). Then, the compensation current is calculated as the sum of compensation harmonic currents as

$$i_{q,comp} = \sum_n \frac{T_{comp,n}}{1.5 P_n \psi_a} \cos\left(n\theta_{out} + \phi_{comp,n}\right) \tag{18}$$

where $i_{q,comp}$ is the compensation current. Then, the q-axis current reference which is the input of the q-axis PI controller can be calculated from the constant q-axis current command and compensation current as

$$i_{q,ref} = i_q^* + i_{q,comp} \tag{19}$$

where i_q^* is the q-axis current command. As the compensation current is injected into the q-axis current, the compensation torque includes the torque ripple for suppressing the misalignment torque ripple.

IV. Experimental Results

In this section, several experiments were conducted to verify the proposed method. The descriptions about experiments are shown in Fig. 9. Each experiment starts with conditions of constant q-axis current and constant load torque. In Section IV.B, a verification of estimation method for misalignment torque ripple was described by comparing the measured and estimated misalignment torque ripple. In Section IV.C, an effectiveness of the HCIM was described. The resultant torque ripple according to the amplitude and phase of injected harmonic current were measured to verify the effectiveness of HCIM. Finally, the proposed MPC-HCIM was verified in Section IV.D.

A. Experimental Setup

The experimental setup is shown in Fig. 10. The actuator, torque sensor, and the brake load are connected in series. The specifications of the actuator are shown in Table I. The SPMSM is driven by feedback from a 12-bit incremental encoder which is attached to the motor shaft. In addition, the SPMSM is controlled by DSP of Texas Instrument (TI) TMS320F28377D and the switching frequency of the inverter is set to 10 kHz.

Prior to examining the characteristics of the SPMSM, the torque ripple component that affects the rotor dynamics of the actuator was analyzed using the frequency response of the actuator. Fig. 11 shows the frequency response of the mechanical system referred in the output shaft of the gearbox. As shown in the bode plot, the bandwidth of the mechanical system is calculated as 43.4 Hz. Since the bandwidth is defined as the frequency range where the magnitude of the closed-loop gain does not drop below -3 dB, the torque ripple with frequency above the

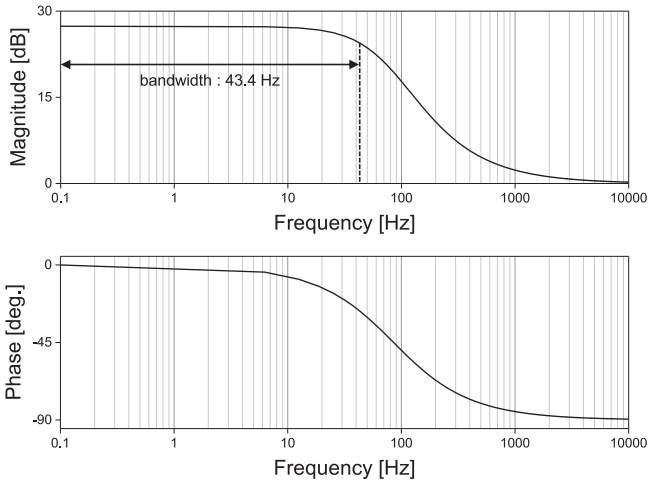

Fig. 11. Frequency response of mechanical system referred in output shaft of the gearbox. Magnitude, bandwidth, and phase of the frequency response.

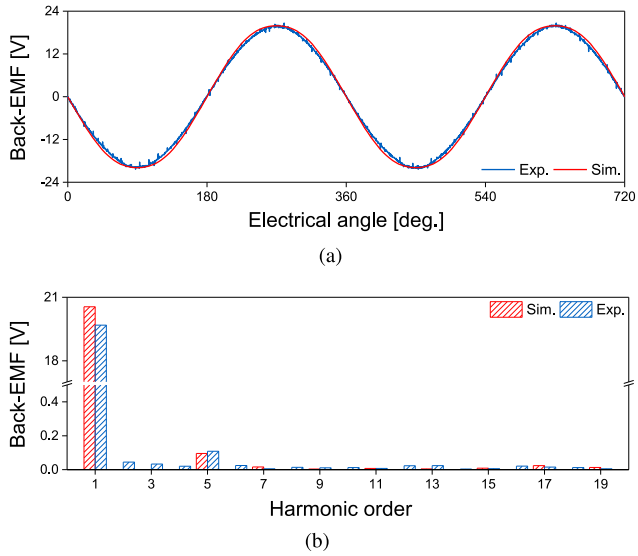

Fig. 12. Comparison of the simulated and measured Back-EMF. (a) Waveform and (b) harmonic analysis of the Back-EMF.

bandwidth has little effect on the speed ripple. Therefore, the torque ripple caused by PWM harmonics does not affect to the system dynamics because the switching frequency of inverter is set to 10 kHz. The harmonic components in q-axis current can be caused by the performance of the current controller, which affects to the torque ripple. In order to exclude the influence of the control gain on the torque ripple, the gain of the current controller was well tuned to converge to the target value without overshoot.

In order to test the proposed method, the SPMSM must have appropriate characteristics. To test the proposed method effectively, the electromagnetic torque ripple should be generated only by the injected harmonic currents. Therefore, the SPMSM in the actuator have to generate a small electromagnetic torque ripple. The back-electromotive force (Back-EMF) and torque ripple of SPMSM are used to verify the suitablity of the SPMSM. The Back-EMF was verified through electromagnetic FEA and experiment, but the torque ripple was verified only using FEA because the SPMSM cannot be tested with dynamometer solely due to the structure of the actuator. Fig. 12(a) and Fig. 12(b) show the results of waveform and harmonic analysis of the Back-EMF at 1000 rpm. Since the SPMSM was designed to make the Back-EMF sinusoidal, the SPMSM includes small harmonic components of the Back-EMF. The total harmonic distortion (THD) of the simulated Back-EMF was 0.50%, and the measured Back-EMF was 0.78%. Fig. 13 shows the electromagnetic torque of the SPMSM when the rated q-axis current is excited. The averaged electromagnetic torque was 0.5 Nm and the torque ripple was 1.71%. Therefore, the SPMSM used in the actuator is suitable for testing the HCIM.

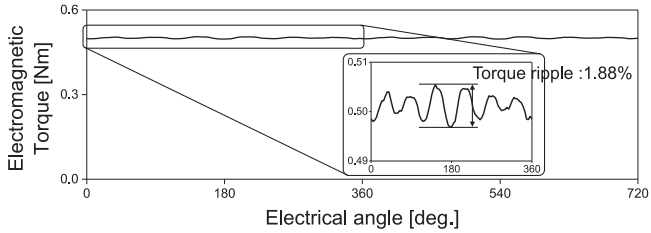

Fig. 13. Simulated torque ripple of the SPMSM.

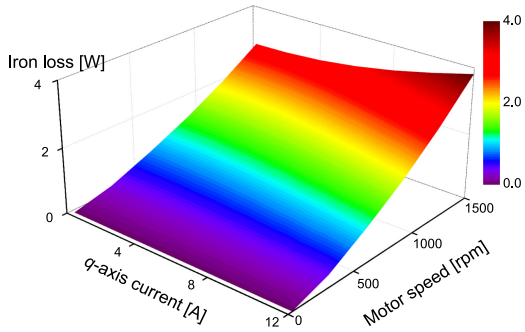

Fig. 14. Calculated iron loss of SPMSM according to the q-axis current and motor speed.

B. Verification of Misalignment Torque Ripple Estimation

In order to use the estimation method of misalignment torque ripple for predictive model, the verification have to be conducted prior to test the proposed MPC-HCIM. The misalignment torque ripple can be obtained from the estimation method of (9). Since the rotating speed is fluctuated by the misalignment torque ripple, iron loss of the SPMSM according to the q-axis current and speed is necessary to use the estimation method. The iron loss was calculated by using the electromagnetic FEA and it has high accuracy compared with the experimental results because it uses the measured iron loss data [26]. The calculated iron loss is shown in Fig. 14. Then, the misalignment torque ripple can be calculated considering the friction coefficient and iron loss. The misalignment torque ripple obtained from the torque sensor and estimation method are compared in Fig. 15(a) and

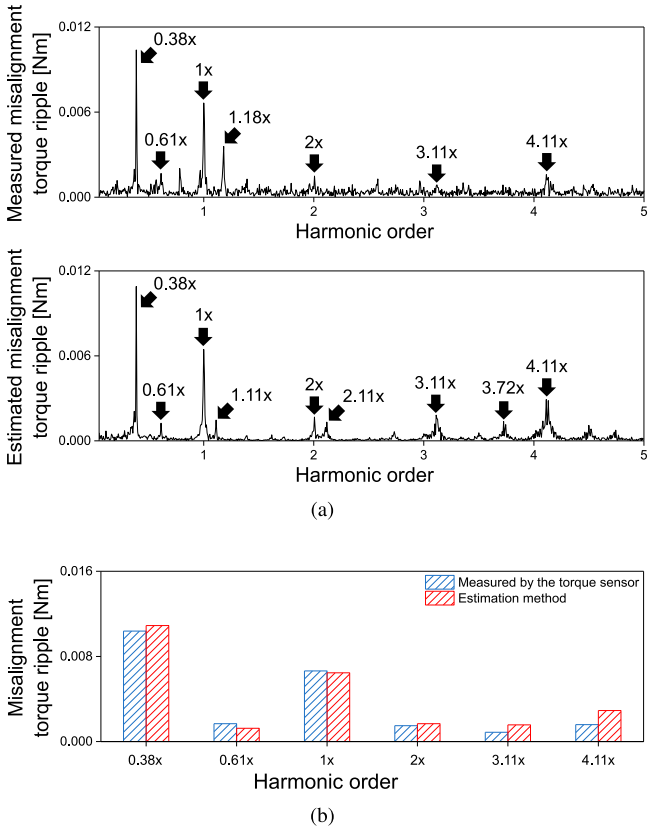

Fig. 15. Verification of effectiveness of the estimation method. (a) Measured and estimated misalignment torque ripple, and (b) the comparison results.

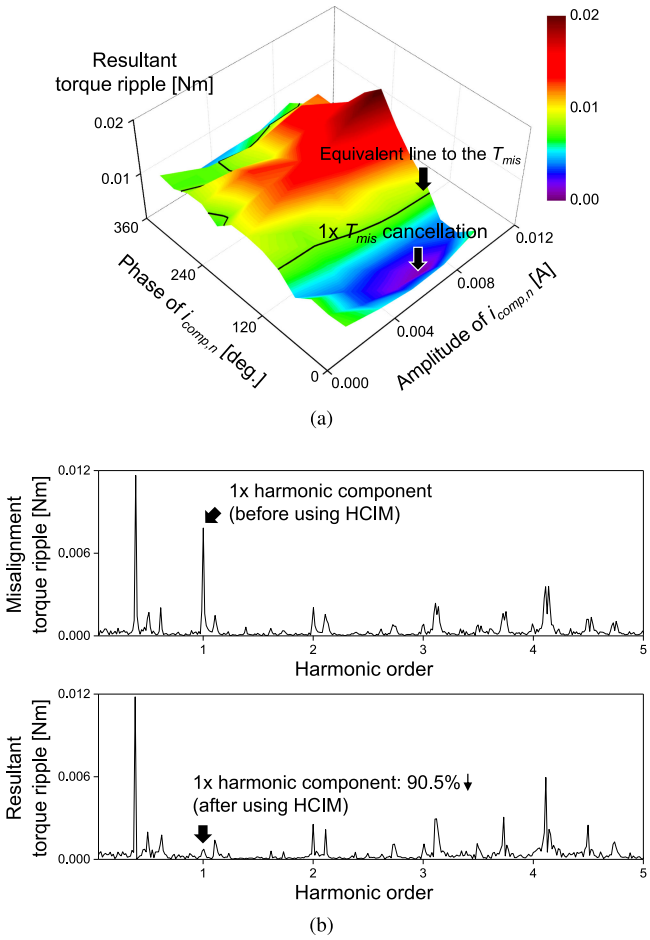

Fig. 16. Resultant torque ripple with 1st harmonic current injection. (a) The resultant torque according to the amplitude and phase of 1st harmonic current, and (b) effectiveness of the HCIM for 1st harmonic component.

Fig. 15(b). The fundamental component of misalignment torque ripple is equivalent to the frequency of output shaft. As shown in Fig. 15(a), the major harmonic components having an amplitude above 10% compared to the harmonic component that has largest amplitude was confirmed as the 0.38th, 0.61th, 1st, 2nd, 3.11th and 4.11th orders. It can be observed that the major harmonic components were well predicted by using the estimation method. However, unexpected torque ripple may occur due to the measurement error such as 1.18th harmonic order. The accuracy of the predicted major harmonic components was evaluated using NRMSE, and the estimation method was evaluated with an accuracy of 6.2%.

C. Effectiveness of the Harmonic Current Injection Method

Before verifying the proposed MPC-HCIM, experiments were conducted to verify the effectiveness of the HCIM. To verify the effect of the HCIM, the trend of resultant torque ripple was estimated according to the amplitude and phase of harmonic current as shown in Fig. 16(a). The experiments were conducted only for the 1st harmonic order referred in output shaft. It can be observed that the 1st harmonic component of misalignment torque ripple is completely cancelled by injecting the optimal harmonic current. As a result of injecting the optimal 1st harmonic current, the 1st resultant torque ripple was suppressed by 90.5% as shown in Fig. 16(b). Since it is inefficient to search the appropriate amplitude and phase of the compensation torque for every harmonic orders manually, the MPC is used to search those parameters for effective HCIM .

TABLE II
EXPERIMENTAL CONDITIONS TO VERIFY THE EFFECTIVENESS OF MPC-HCIM

Experiment	Load torque [Nm]	Motor speed [rpm]
Experiment 1	1 (12.5% of rated torque)	700 (63% of max. speed)
Experiment 2	2 (25% of rated torque)	700 (63% of max. speed)

D. Verification of Proposed MPC-HCIM for Misalignment Torque Ripple Suppression

In this section, experiments were conducted to verify the effectiveness of the proposed MPC-HCIM. The experiment results show the q-axis current, waveform and harmonic analysis result of misalignment torque before and after applying MPC-HCIM. The experiments were conducted after rotating the actuator for 30 minutes to minimize the effect of the temperature change in the permanent magnets, conductors, bearing and lubrication of the gearbox.

The experiments were conducted to verify the effectiveness of the proposed method under various load conditions, as shown

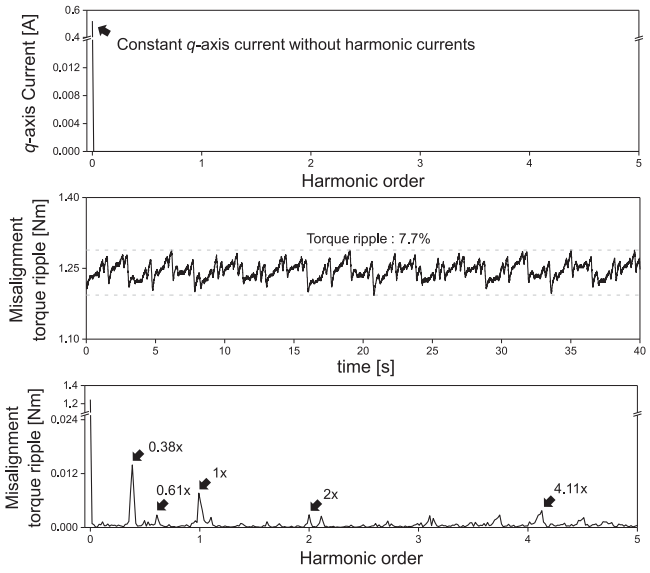

Fig. 17. Experimental results without proposed MPC-HCIM according to the conditions of experiment 1.

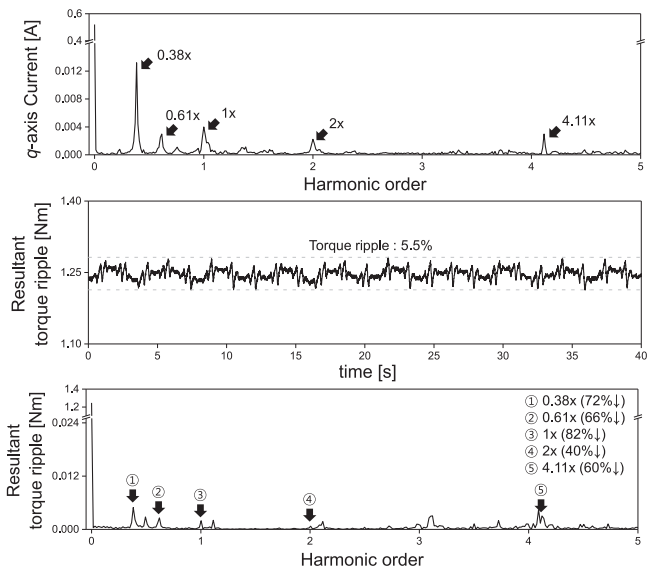

Fig. 18. Experimental results with proposed MPC-HCIM according to the conditions of experiment 1.

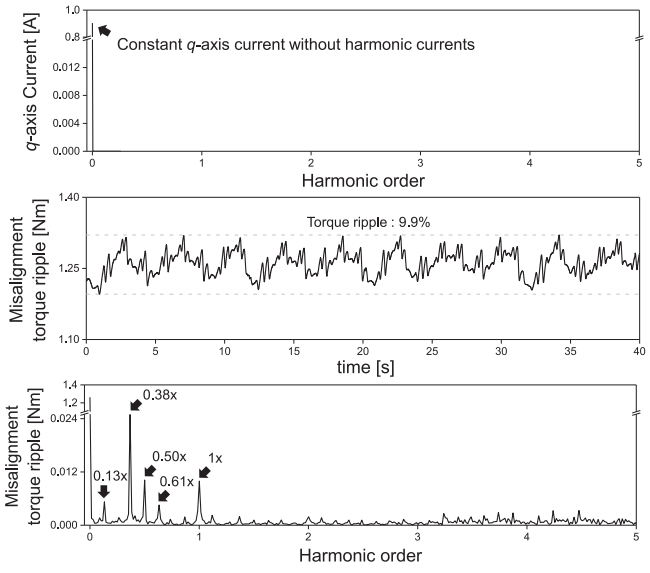

Fig. 19. Experimental results without proposed MPC-HCIM according to the conditions of experiment 2.

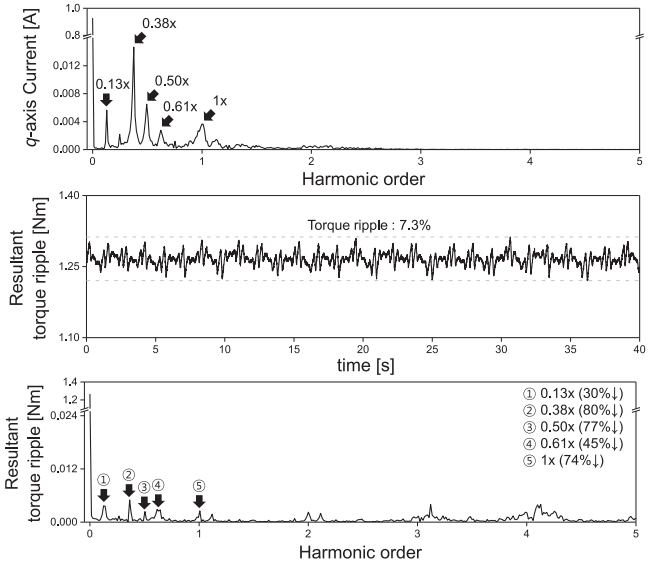

Fig. 20. Experimental results with proposed MPC-HCIM according to the conditions of experiment 2.

in Table II. The experiments were conducted under load torque of 1 Nm and 2 Nm which are 12.5% and 25.0% of the rated torque, respectively. The rotating speed of motor shaft was set to be 700 rpm which is 63% of the maximum speed.

Fig. 17 shows the experiment results without MPC-HCIM according to the conditions of experiment 1. Since the largest amplitude of misalignment torque ripple was estimated in 0.38th harmonic order, the harmonic orders of the compensation torque were determined as the harmonic orders in which the amplitude of the torque ripple was greater than 20% of the amplitude of the 0.38th harmonic order. Thus, the compensation torque includes the harmonic orders of 0.38th, 0.61th, 1st, 2nd, and 4.11th and the compensation current also includes same harmonic orders. Fig. 18 shows the experiment results with MPC-HCIM. As a result of using the MPC-HCIM, the harmonic currents which have same harmonic order with compensation torque were injected into the q-axis current. Then, the misalignment torque ripple was effectively suppressed in each harmonic order. The overall resultant torque ripple was decreased from 7.7% to 5.5%, and the fundamental component of misalignment torque ripple was significantly reduced by 82%.

Fig. 19 shows the experiment results without MPC-HCIM according to the conditions of experiment 2. As the load torque was increased, q-axis current, magnetic flux density, and core loss of the actuator were increased. Therefore, it can be observed that the amplitude of the misalignment torque ripple was increased compared to the result of experiment 1. Since the

major harmonic orders of the misalignment torque ripple were analyzed as 0.13th, 0.38th, 0.50th, 0.61th, and 1st component, the compensation current also includes same harmonic orders as shown in Fig. 20. As a result of using the MPC-HCIM, the overall resultant torque ripple was reduced from 9.9% to 7.3%, and the misalignment torque ripple was significantly reduced by 80% at 0.38th harmonic component.

V. Conclusion and Future Works

In this paper, a model predictive control based harmonic current injection method has been proposed to suppress misalignment torque ripple. The misalignment torque ripple can be suppressed by using harmonic current injection method. Since the determination for appropriate amplitude and phase of the harmonic currents is inefficient, the MPC is used to implement HCIM efficiently. As a result of using the proposed method, the misalignment torque ripple was suppressed by injecting optimal compensation torque which was calculated by minimizing the cost function of MPC. Therefore, the high degree of precision in torque control can be achieved by using the proposed method despite of using the gearbox with misalignment. In order to achieve the versatile for the proposed method, additional studies should be conducted. The first is to consider the uncertainty of the parameter according to the temperature change. Since the motor parameters are changed by temperature variation, a method considering the temperature variation should be proposed. Second is to consider the delay due to digital control for improving performance of transient-state. Since the proposed method is effective in steady-state, the robust MPC for suppressing the misalignment torque ripple in both steady-state and transient-state will be conducted as a future work.

References

[1] H. J. Park, M. S. Lim, and C. S. Lee, "Magnet shape design and verification for SPMSM of EPS system using cycloid curve," *IEEE Access*, vol. 7, pp. 137207–137216, 2019.

[2] M. Abdelrahem, C. M. Hackl, Z. Zhang, and R. Kennel, "Robust predictive control for direct-driven surface-mounted permanent-magnet synchronous generators without mechanical sensors," *IEEE Trans. Energy Convers.*, vol. 33, no. 1, pp. 179–189, Mar. 2018.

[3] P. Beccue, J. Neely, S. Pekarek, and D. Stutts, "Measurement and control of torque ripple-induced frame torsional vibration in a surface mount permanent magnet machine," *IEEE Trans. Power Electron.*, vol. 20, no. 1, pp. 182–191, Jan. 2005.

[4] J. Piotrowski, "Detecting misalignment on rotating machinery," *Shaft Alignment Handbook*, 3rd ed. FL USA: CRC Press, 2007, pp. 35–87.

[5] K. Lee, C. Lee, S. Hwang, J. Choi, and Y. Bang, "Power-assisted wheelchair with gravity and friction compensation," *IEEE Trans. Ind. Electron.*, vol. 63, no. 4, pp. 2203–2211, Apr. 2016.

[6] B. Bona, M. Indri, and N. Smaldone, "Rapid prototyping of a model-based control with friction compensation for a direct-drive robot," *IEEE/ASME Trans. Mechatronics*, vol. 11, no. 5, pp. 576–584, Oct. 2006.

[7] Y. H. Jung, M. S. Lim, M. H. Yoon, J. S. Jeong, and J. P. Hong, "Torque ripple reduction of IPMSM applying asymmetric rotor shape under certain load condition," *IEEE Trans. Energy Convers.*, vol. 33, no. 1, pp. 333–340, Mar. 2018.

[8] S. S. R. Bonthu, M. T. B. Tarek, and S. Choi, "Optimal torque ripple reduction technique for outer rotor permanent magnet synchronous reluctance motors," *IEEE Trans. Energy Convers.*, vol. 33, no. 3, pp. 1184–1192, Sep. 2018.

[9] C. Lai, G. Feng, K. Mukherjee, and N. C. Kar, "Investigations of the influence of PMSM parameter variations in optimal stator current design for torque ripple minimization," *IEEE Trans. Energy Convers.*, vol. 32, no. 3, pp. 1052–1062, Sep. 2017.

[10] I. Godler, T. Ninomiya, and M. Horiuchi, "Ripple compensation for torque sensors built into harmonic drives," *IEEE Trans. Instrum. Meas.*, vol. 50, no. 1, pp. 117–122, Feb. 2001.

[11] H. Taghirad and P. Belanger, "Torque ripple and misalignment torque compensation for the built-in torque sensor of harmonic drive systems," *IEEE Trans. Instrum. Meas.*, vol. 47, no. 1, pp. 309–315, Feb. 1998.

[12] M. Kermani, R. Patel, and M. Moallem, "Friction identification and compensation in robotic manipulators," *IEEE Trans. Instrum. Meas.*, vol. 56, no. 6, pp. 2346–2353, Dec. 2007.

[13] G. J. Li, K. Zhang, Z. Q. Zhu, and G. W. Jewell, "Comparative studies of torque performance improvement for different doubly salient synchronous reluctance machines by current harmonic injection," *IEEE Trans. Energy Convers.*, vol. 34, no. 2, pp. 1094–1104, Jun. 2019.

[14] G. H. Lee, S. I. Kim, J. P. Hong, and J. H. Bahn, "Torque ripple reduction of interior permanent magnet synchronous motor using harmonic injected current," *IEEE Trans. Magn.*, vol. 44, no. 6, pp. 1582–1585, Jun. 2008.

[15] H. Jia, M. Cheng, W. Hua, W. Zhao, and W. Li, "Torque ripple suppression in flux-switching PM motor by harmonic current injection based on voltage space-vector modulation," *IEEE Trans. Magn.*, vol. 46, no. 6, pp. 1527–1530, Jun. 2010.

[16] B. S. Lee, Z. Q. Zhu, and L. R. Huang, "Torque ripple reduction for 6-Stator/4-Rotor-Pole variable FLux reluctance machines by using harmonic field current injection," *IEEE Trans. Ind. Appl.*, vol. 53, no. 4, pp. 3730–3737, Jul./Aug. 2017.

[17] S. H. Park, J. C. Park, S. W. Hwang, J. H. Kim, H. J. Park, and M. S. Lim, "Suppression of torque ripple caused by misalignment of the gearbox by using harmonic current injection method," *IEEE/ASME Trans. Mechatronics*, vol. 25, no. 4, pp. 1990–1999, Aug. 2020.

[18] S. Kouro, P. Cortes, R. Vargas, U. Ammann, and J. Rodriguez, "Model predictive controll-a simple and powerful method to control power converters," *IEEE Trans. Ind. Electron.*, vol. 56, no. 6, pp. 1826–1838, Jun. 2009.

[19] C. S. Lim, E. Levi, M. Jones, N. A. Rahim, and W. P. Hew, "FCS-MPC-Based current control of a five-phase induction motor and its comparison with PI-PWM control," *IEEE Trans. Ind. Electron.*, vol. 61, no. 1, pp. 149–163, Jan. 2014.

[20] V. Yaramasu and B. Wu, *Model Predictive Control of Wind Energy Conversion System*. Hoboken, NJ, USA: Wiley, 2016.

[21] S. Kouro, B. Rocca, P. Cortes, S. Alepuz, B. Wu, and J. Rodriguez, "Predictive control based selective harmonic elimination with low switching frequency for multilevel converters," in *Proc. IEEE Energy Conv. Congr. Expo.*, Sep. 2009, pp. 3130–3136.

[22] R. Aguilera *et al.*, "Selective harmonic elimination model predictive control for multilevel power converters," *IEEE Trans. Power Electron.*, vol. 32, no. 3, pp. 2416–2426, Mar. 2017.

[23] A. W. Lees, "Misalignment in rigidly coupled rotors," *J. Sound Vib.*, vol. 305, no. 1–2, pp. 261–271, Aug. 2007.

[24] J. Chacon, E. Andicoberry, V. Kappatos, G. Asfis, T. Gan, and W. Balachandran, "Shaft angular misalignment detection using acoustic emission," *Appl. Acoust.*, vol. 85, pp. 12–22, Nov. 2014.

[25] A. Bellini, A. Yazidi, F. Filippetti, C. Rossi, and G. A. Capolino, "High frequency resolution techniques for rotor fault detection of induction machines," *IEEE Trans. Ind. Electron.*, vol. 55, no. 12, pp. 4200–4209, Dec. 2008.

[26] D. M. Kim, J. W. Chin, J. P. Hong, and M. S. Lim, "Performance prediction of surface-mounted permanent magnet synchronous motor based on ring specimen test result," *IET Electr. Power Appl.*, vol. 13, no. 9, pp. 1280–1286, Sep. 2019.

Soo-Hwan Park received the bachelor's degree in mechanical engineering from Hanyang University, Seoul, South Korea, in 2014. He is currently working toward the Ph.D. degree in automotive engineering. From 2019 to 2020, he was with the Korea Institute of Industrial Technology, Daegu, South Korea. His research interests include electromagnetic field analysis, design and optimization of electric machines for automotive and robotics applications, and electric machine drive for industrial applications.

Jin-Cheol Park received the bachelor's degree in electrical engineering from Chungbuk National University, Cheongju, South Korea, in 2015 and the master's degree in 2017 from Hanyang University, Seoul, South Korea, where he is currently working toward the Ph.D. degree in automotive engineering. His research interests include electric machine design for automotive and numerical analysis of electromagnetics.

Sung-Woo Hwang received the bachelor's degree in mechanical engineering in 2013 from Hanyang University, Seoul, South Korea, where he is currently working toward the Ph.D. degree in automotive engineering. His research interests include electric machine design for automotive and robot applications, and numerical analysis of electromagnetics.

Jae-Hyun Kim received the bachelor's degree in mechanical engineering in 2017 from Hanyang University, Seoul, South Korea, where he is currently working toward the Ph.D. degree in automotive engineering. His research interests include the design and the analysis of vibration and noise of electric machines.

Myung-Seop Lim received the bachelor's degree in mechanical engineering, from Hanyang University, Seoul, South Korea, in 2012, and the master's and Ph.D. degrees in automotive engineering from Hanyang University in 2014 and 2017, respectively.

From 2017 to 2018, he was a Research Engineer with Hyundai Mobis, Yongin, South Korea. From 2018 to 2019, he was an Assistant Professor with Yeungnam University, Daegu, South Korea. Since 2019, he has been with Hanyang University, Seoul, where he is currently an Assistant Professor.

His research interests include electromagnetic field analysis and electric machinery for mechatronics systems, such as automotive and robot applications.